THE JOURNAL OF BIOLOGICAL CHEMISTRY VOL. 283, NO. 9, pp. 5780–5789, February 29, 2008

Calcium Homeostasis and Mitochondrial Dysfunction in Striatal Neurons of Huntington Disease*[S]

Received for publication, June 7, 2007, and in revised form, December 17, 2007 Published, JBC Papers in Press, December 21, 2007, DOI 10.1074/jbc.M704704200

Dmitry Lim[‡§], Laura Fedrizzi[‡§¶], Marzia Tartari[‖], Chiara Zuccato[‖], Elena Cattaneo[‖], Marisa Brini[§¶], and Ernesto Carafoli[‡§1]

From the [‡]Venetian Institute of Molecular Medicine, Via Orus 2, 35129 Padua, Italy, the Departments of [§]Biochemistry and [¶]Experimental Veterinary Science, University of Padua, Viale Colombo 3, 35131 Padua, Italy, and the [‖]Department of Pharmacological Sciences, University of Milan, Milan, Italy

Dysfunctions of Ca^{2+} homeostasis and of mitochondria have been studied in immortalized striatal cells from a commonly used Huntington disease mouse model. Transcriptional changes in the components of the phosphatidylinositol cycle and in the receptors for *myo*-inositol trisphosphate-linked agonists have been found in the cells and in the striatum of the parent Huntington disease mouse. The overall result of the changes is to delay *myo*-inositol trisphosphate production and to decrease basal Ca^{2+} in mutant cells. When tested directly, mitochondria in mutant cells behave nearly normally, but are unable to handle large Ca^{2+} loads. This appears to be due to the increased Ca^{2+} sensitivity of the permeability transition pore, which dissipates the membrane potential, prompting the release of accumulated Ca^{2+}. Harmful reactive oxygen species, which are produced by defective mitochondria and may in turn stress them, increase in mutant cells, particularly if the damage to mitochondria is artificially exacerbated, for instance with complex II inhibitors. Mitochondria in mutant cells are thus peculiarly vulnerable to stresses induced by Ca^{2+} and reactive oxygen species. The observed decrease of cell Ca^{2+} could be a compensatory attempt to prevent the Ca^{2+} stress that would irreversibly damage mitochondria and eventually lead to cell death.

Huntington disease (HD)[2] is a fatal disease characterized by chorea and psychiatric disturbance (1) caused by the expansion of CAG repeats in the first exon of the gene encoding huntingtin (Htt). In the normal gene, the repeats specify a stretch of up to 36 Gln in the N-terminal region of Htt. In the disease, the poly-Q tract is longer, and the mutant protein becomes harmful to cells. Htt is expressed ubiquitously in human tissues, but its mutation is particularly harmful to cortical and striatal medium size spiny neurons (MSNs) (2). The reasons for the specific damage to these neurons is an open problem in HD research, which reflects the incomplete knowledge on the function(s) of Htt. Htt interacts with several proteins in neurons, and plays roles in processes like axonal transport, regulation of transcription, exocytosis, calcium homeostasis, and prevention of apoptosis (3). It is easy to see that dysfunctions in any one of these processes, *e.g.* in Ca^{2+} homeostasis, could be involved in the ethiology of HD (4). As for the molecular mechanisms of the harmful effects of the mutated protein, the idea is now gaining ground that the extended poly-Q tract, cleaved off from Htt, causes the transcriptional dysfunction of genes that are essential for neuronal survival. Htt, however, could also have non-transcriptional effects.

Mitochondrial defects may have a causative role in neurodegenerative diseases, and are considered important in HD ethiology (5). They have indeed been found in the brain of HD patients (6) and in the striatal and other cells of animal HD models (7–9). The defective mitochondrial component has been suggested to be complex II of the respiratory chain. The suggestion is supported by experimental findings, for example the demonstration that the specific inhibitor 3-nitropropionic acid (3-NPA) induces a degeneration of rat striatal neurons that mimics that seen in the disease (10, 11). The alterations in Ca^{2+} homeostasis commonly observed in neuronal damage (12, 13) could also have a role in the HD ethiology. In neurons, the mobilization of Ca^{2+} from the endoplasmic reticulum (ER) through channels modulated by $InsP_3$ produced in the phosphatidylinositol (PI) cycle is an important component of Ca^{2+} homeostasis. In the striatal neurons studied here the cycle is only activated by two plasma membrane agonists: ATP and bradykinin (BK). ATP produces $InsP_3$ through fast acting ionotropic (P2X) receptors, and slower acting, G_q protein-coupled P2Y receptors (14). The receptors for BK are all coupled to G_q proteins (15). The alterations of Ca^{2+} homeostasis, if resulting for instance in the increased release of Ca^{2+} from the ER, could exacerbate the mitochondrial dysfunction, as the complex II defect would limit the ability of the respiratory chain to increase activity, presumably making mitochondria peculiarly unable to retain the Ca^{2+} they have accumulated (16). However, the inability to retain Ca^{2+} could also be due to the increased pro-

* This work was supported by the European Union FP6 Integrated Project NeuroNE (to E. C. and E. C.), Telethon Foundation Project GGP04169 (to M. B.), and the Italian Ministry of University and Research (PRIN 2005, to M. B. and the FIRB 2001, to E. C.). The costs of publication of this article were defrayed in part by the payment of page charges. This article must therefore be hereby marked "*advertisement*" in accordance with 18 U.S.C. Section 1734 solely to indicate this fact.

[S] The on-line version of this article (available at http://www.jbc.org) contains supplemental Table S1.

[1] To whom correspondence should be addressed: Venetian Institute of Molecular Medicine, Via Orus 2, 35129 Padua, Italy. Tel.: 39-049-8276137; Fax: 39-049-8276125; E-mail: ernesto.carafoli@unipd.it.

[2] The abbreviations used are: HD, Huntington disease; $InsP_3$, *myo*-inositol trisphosphate; ROS, reactive oxygen species; IMPA1, *myo*-inositol monophosphatase 1; PLCβ, phospholipase Cβ; PGC-1α, PPARγ coactivator 1α; Gpx, glutathione peroxidase; SOD, superoxide dismutase; TMRM, tetramethylrhodamine methyl ester; FCCP, carbonyl cyanide trifluoromethoxyphenylhydrazone; AEQ, aequorin; Q-RT, quantitative real-time; BK, bradykinin; ER, endoplasmic reticulum.

pensity of the permeability transition pore to open: recent findings have shown that the membrane potential ($\Delta\psi_m$) in mitochondria of cells expressing mutant huntingtin is peculiarly sensitive to Ca^{2+} (17), and that poly-Q constructs de-energize isolated mitochondria exposed to Ca^{2+} (17).

Reactive oxygen species (ROS) also damage mitochondria, *i.e.* they dissipate the $\Delta\psi_m$, and are thus frequently mentioned in the pathogenesis of neurodegenerative diseases. They are produced by defective mitochondria, and in HD neurons they could be generated by the dysfunction of complex II. This is suggested by the finding that in normal neurons they increase following the inhibition of the complex by 3-NPA (18). An interesting development in the area of ROS has been the observation (19, 20) that the striatal neurons are particularly sensitive to the mitochondrial damage caused by the lack of a co-activator of the transcription of the genes for ROS-scavenging enzymes (acronym PGC-1α). PGC-1α regulates a number of cell processes, among them the response of mitochondria to oxidative stress. PGC-1α is down-regulated in the striatum of HD patients (21), in striatal neurons of HD knock-in mice, and even in the immortalized striatal cells used in this work. Mutant Htt has been found to associate with the promoter of the PGC-1α gene, decreasing its transcription. As a result, the transcription of ROS-scavenging enzymes is down-regulated, and the concentration of ROS in the neurons increases. These important observations were reinforced by the finding that striatal neurons from HD knock-in mice were resistant to 3-NPA when expressing exogenous PGC-1α (22).

To integrate the effects of Ca^{2+} and ROS in the neuronal damage in HD, we have studied their dynamics in a commonly used HD model, *i.e.* in immortalized striatal neuron precursor cells from a HD knock-in mouse model (KI-Hdh^{Q111}) (23), and in the striata of the parent model mice. The immortalization affects cells growth and differentiation, but important biochemical mechanisms of primary brain cells are faithfully conserved in the cell line, and have allowed the discovery of interesting paths affected by the Htt mutation (reviewed in Ref. 24). We have found that the expression of the enzymes of the PI cycle, and of the receptors of the two agonists that activate it in this cell model, was profoundly altered in the mutant cells and in the striatum of the parent mice. As a result, the basal Ca^{2+} level in the cells decreased, and the production of $InsP_3$ that would mediate its liberation in response to agonist stimulation, was delayed. The handling of Ca^{2+} by mitochondria was studied directly within the mutant cells, and found to be compromised, but only when the Ca^{2+} loads presented to the mitochondria were large. The inability of mitochondria to absorb the Ca^{2+}-induced stress was exacerbated if the damage to complex II, which could be possibly compromised in the cell line, was artificially augmented with inhibitors. The transcription of ROS-degrading enzymes was also examined: in three clones of the mutant cells, which were examined, it was found to be consistently up-regulated. That of PGC-1α, instead, varied in the three mutant clones. The concentration of ROS in the mutant cells did not differ significantly from the controls, but increased markedly in both cell types if mitochondria were artificially damaged, for instance by exposing them to the complex II inhibitor 3-NPA. The increase was much more pronounced in mutant cells. Thus, mitochondria in mutant cells (and, as is plausible to assume, in HD neurons) appear to be peculiarly vulnerable to stress. The changes in Ca^{2+} homeostasis in the cells studied here could reflect a compensatory attempt to limit, or at least to delay, mitochondrial damage.

EXPERIMENTAL PROCEDURES

Cell Cultures

Clonal striatal cell lines established from E14 striatal primordia of KI-Hdh^{Q111} and WT-Hdh^{Q7} littermate mouse embryos were described previously (23). The cells were grown in Dulbecco's modified essential medium (EuroClone, Milan, Italy) supplemented with 10% fetal bovine serum (EuroClone), 2 mM glutamine, 10 units/ml penicillin, 100 μg/ml streptomycin. They were maintained at the permissive temperature (33 °C) in a humidified incubator with 5% CO_2.

Chemicals

Stock solutions in water of ATP (100 mM) and BK (1 mM) (Sigma, St. Louis, MO) were prepared, aliquoted, and stored at −20 °C. Submaximal final concentrations of agonists were used in the experiments (100 μM ATP and 100 nM BK). Stock solutions of FCCP (10 mM, Sigma) and cyclosporin A (CsA, 83.1 mM) were prepared in ethanol. Final concentration of ethanol in working solutions did not exceed 0.2%.

Ca^{2+} Measurements

Aequorin—STHdh^{Q7} and STHdh^{Q111} cells were transfected with plasmid DNAs encoding cytosolic (cytAEQ), mitochondrial (mtAEQ), or endoplasmic reticulum (erAEQ) aequorin using TransFectin Lipid Reagents (Bio-Rad Laboratories, Hercules, CA). Ca^{2+} measurements were performed as described elsewhere (25). All measurements were carried out at 37 °C. The light signal was collected and stored in an IBM-compatible computer for further analysis. The luminescence data were converted off-line into $[Ca^{2+}]$ values, using a previously described computer algorithm (25).

Fura-2—For Fura-2 measurements cells were plated on 24-mm coverslips in 6-well plates at a density of 400,000 cells per well. 24-h later, cells were loaded with 5 μM Fura-2 AM (Invitrogen, San Giuliano Milanese, Italy) in KRB (Krebs-Ringer modified buffer: 125 mM NaCl, 5 mM KCl, 1 mM Na_3PO_4, 1 mM $MgSO_4$, 5.5 mM glucose, 20 mM HEPES, pH 7.4) supplemented with 1 mM Ca^{2+} (KRB-Ca) for 30 min at room temperature. After washing with KRB-Ca cells were left for additional 30 min at room temperature for de-esterification of Fura-2. The coverslip was then placed on the stage of a Zeiss Axiovert 100 epifluorescence microscope, equipped with a 16-bit digital CCD videocamera (Micromax, Princeton Instruments, Trenton, NJ). Samples were alternatively illuminated at 340 and 380 nm, and the emitted light (filtered with an interference filter centered at 510 nm) was collected by the camera. Images were acquired using the MetaFluor software (Universal Imaging, West Chester, PA). The ratio values (1 ratio image/sec) were calculated off-line, after background subtraction from each single image. To quantify the differences in the peaks of the responses the data were normalized using the formula $F_i(F_0\text{-}F_i)$

commonly used in experiments of this type. The data on basal Ca^{2+} levels are expressed as 340/380 ratio values.

$InsP_3$ Quantification

For $InsP_3$ quantification, cells were stimulated with ATP (100 μM) and/or BK (100 nM). The reaction was arrested at the indicated time-points with one-third volume of 1.05% PCA (Sigma). 1-h later extracts were collected and subjected to an AlphaScreen $InsP_3$ assay according to the manufacturer's protocol (AlphaScreen-GST and AlphaScreen $InsP_3$ supplement, Perkin Elmer, Wellesley, MA).

Membrane-permeable $InsP_3$

A 10 mM stock solution of D-2,3-*o*-isopropylidene-*myo*-inositol 1,4,5-trisphosphate-hexakis(propionoxymethyl) ester (i$InsP_3$/PM, SiChem, Bremen, Germany) in Me_2SO was prepared, aliquoted, and stored at −20 °C. STHdh^{Q7} and STHdh^{Q111} cells were loaded with Fura-2 and i$InsP_3$/PM was added at a final concentration of 100 μM. Fura-2 images were collected every 3 s and the 340/380 ratio values were normalized as described above.

RNA Preparation and Reverse Transcription

STHdh^{Q7} and STHdh^{Q111} cells were plated in 100-mm dishes and grown to 80–90% confluency. They were washed three times with cold phosphate-buffered saline and collected with 1 ml of TRIzol reagent (Invitrogen). Total RNA was extracted according to the manufacturer's protocol. Striata from KI-Hdh^{Q111} and WT-Hdh^{Q7} mice were dissected, homogenized in 1 ml of TRIzol reagent, and total RNA was isolated according to the manufacturer's instructions. 1 μg of total RNA was reverse-transcribed using Moloney murine leukemia virus reverse transcriptase (Invitrogen) according to the manufacturer's protocol.

Primers Design and Q-RT-PCR

Specific oligonucleotide primers were designed using Primer3 software (see supplemental Table S1). Q-RT-PCR was performed on a Rotor-Gene 3000 platform (Corbet Research, Sydney, Australia). An amount of cDNA corresponding to 1–10 ng of total RNA was amplified in 25 μl of a mixture containing 12.5 μl of Platinum SYBR Green qPCR SuperMix-UGD (Invitrogen), 2 μl of primers mixture (2.5 μM each). The PCR cycling parameters were: 94 °C for 7 min, 45 cycles of 94 °C for 30 s, 55 °C for 30 s, and 72 °C for 15 s. The relative amount of amplified DNA was calculated as described (26) using hypoxanthine-guanine phosphoribosyltransferase mRNA as endogenous control.

Measurement of Mitochondrial Membrane Potential ($\Delta\psi_m$) and of ROS

The TMRM "diffusion" method was used, which is adequate for the comparison of the $\Delta\psi_m$ between two populations of cells (27). The cells were loaded with 10 nM TMRM for 30 min at 37 °C in KRB containing 1 mM Ca^{2+}. TMRM fluorescence was registered at 510 nm using an Olympus F-View II CCD camera mounted on an Olympus IX-81 microscope equipped with ×40 Uplan FLN objective (Olympus, Tokyo, Japan). The TMRM fluorescence intensity was analyzed off-line using MetaMorph software (Universal Imaging). In the experiments with FCCP, ROIs were positioned across the peripheral cell area, and the standard deviation of TMRM fluorescence was analyzed using MetaMorph software before and after FCCP addition. To measure ROS, STHdh^{Q7} and STHdh^{Q111} cells were treated with 3-NPA (10 mM for 40 h), and loaded with 10 μM 2′,7′-dichlorodihydrofluorescein diacetate acetyl ester (Invitrogen) for 30 min at 37 °C in 100 μl of KRB containing 1 mM Ca^{2+} followed by 30 min of de-esterification. Fluorescence was measured in a Fluoroskan spectrophotometer (Ascent FL, Labsystems, Thermo Electron, Waltham, MA). After background subtraction, the data were normalized to the cell number obtained by counting of nuclei stained by Hoechst 33258 (Sigma).

Lentiviral Transduction with mitAEQ and Measurement of Mitochondrial Ca^{2+} Uptake

To produce plasmid pLV-mitAEQ-IRES-EGFP, mitochondrial AEQ was first subcloned in a pIRES2-EGFP (Clontech, Mountain View, CA) vector, then a cassette containing mitAEQ-IRES-EGFP was transferred to a pRRLsin.PPTs.hCMV.GFPpre lentiviral vector. The resulting construct was denominated as pLV-mtAEQ. Lentiviral particles were produced as described elsewhere (28). The desired lentiviral titer was obtained by infecting STHdh^{Q7} and STHdh^{Q111} cells with serial dilutions of the lentiviral stock. The minimal dilution adequate for 100% infection was used. 48–96 h after the infection AEQ was reconstituted as described in a section above. The cells were permeabilized with an intracellular buffer (100 mM KCl, 1 mM KH_2PO_4, 5 mM sodium succinate, 1 mM $MgCl_2$, 1 mM ATP, 20 mM HEPES; pH 7.0) supplemented with 10 μM digitonin and 50 μM EGTA. Cells were then perfused with Ca^{2+}-EGTA buffers containing the indicated concentrations of free Ca^{2+} (1.6–71 μM). FCCP (Sigma) was added in perfusion solutions at the indicated concentrations. A WebMaxLight software was used to prepare the Ca^{2+}-EGTA buffers.

Caspase Activity Measurement

Cells were plated in 60-mm dishes at the density of 1.2 million cells per dish. 24 h after plating, the cells were treated with 10 μM staurosporin for 6 h. The activity of caspase-3 was detected with the Caspase-3 Colorimetric Activity Assay kit (Chemicon International, Temecula, CA) according to the manufacturer's instructions.

RESULTS

$InsP_3$-linked Ca^{2+} Dynamics in Striatal Cells—The plasma membrane of striatal cells contains P2Y receptors (29). They were challenged with ATP in a medium supplemented with 100 μM EGTA to exclude Ca^{2+} penetration through ionotropic P2X receptors (which are also present in the cells) and store-operated channels. ATP induced a rapid cytoplasmic Ca^{2+} increase in STHdh^{Q7} (control) cells peaking at 1.62 ± 0.17 μM (Fig. 1*A*), and decaying to base line in about 50 s. In STHdh^{Q111} (mutant) cells the peak was much lower (0.67 ± 0.15 μM, $p = 61e\text{-}8$, Fig. 1*A*). The dynamics of the mitochondrial Ca^{2+} pool was explored directly with mtAEQ: the peak of the transient triggered by ATP was much higher in STHdh^{Q7} than in

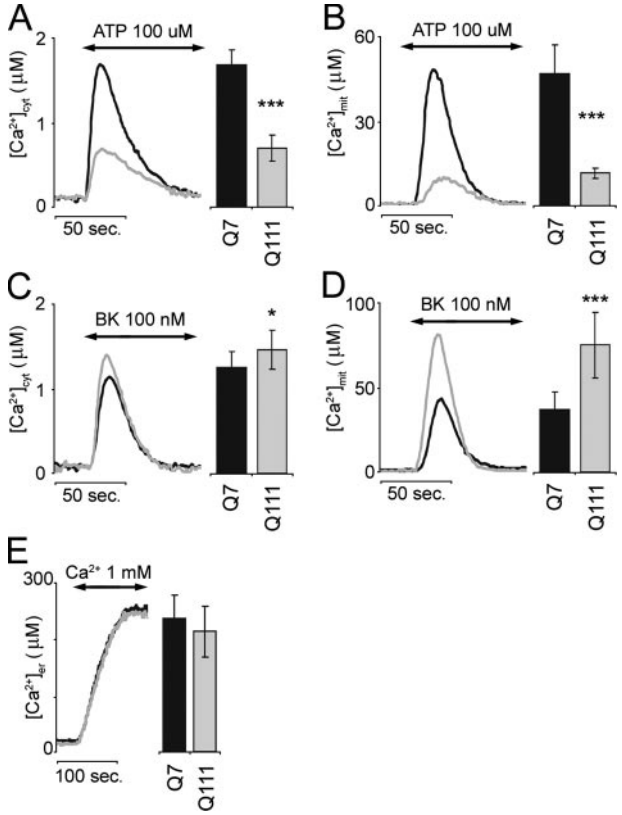

FIGURE 1. **Ca^{2+} dynamics in ST*Hdh*^{Q7} and ST*Hdh*^{Q111} cells stimulated with ATP and BK.** ST*Hdh*^{Q7} (*black traces* and *bars*) and ST*Hdh*^{Q111} (*gray traces* and *bars*) cells expressing cytAEQ (*A* and *C*) or mtAEQ (*B* and *D*) were stimulated with 100 μM ATP (*A* and *B*) or 100 nM BK (*C* and *D*). The data represent the mean ± S.D. of 8–22 measurements. *E*, ST*Hdh*^{Q7} cells (Q7, *black trace* and *bar*) and ST*Hdh*^{Q111} cells (Q111, *gray trace* and *bar*) expressing erAEQ were reconstituted with coelenterazine in KRB buffer containing 100 μM EGTA, and then the solution was changed to KRB supplemented with 1 mM Ca^{2+}. The steady-state Ca^{2+} level in the ER lumen did not differ significantly between Q7 and Q111 cells. The data represent the mean ± S.D. of 10–15 measurements. The differences were significant at $p < 0.05$, *; and $p < 0.001$, ***.

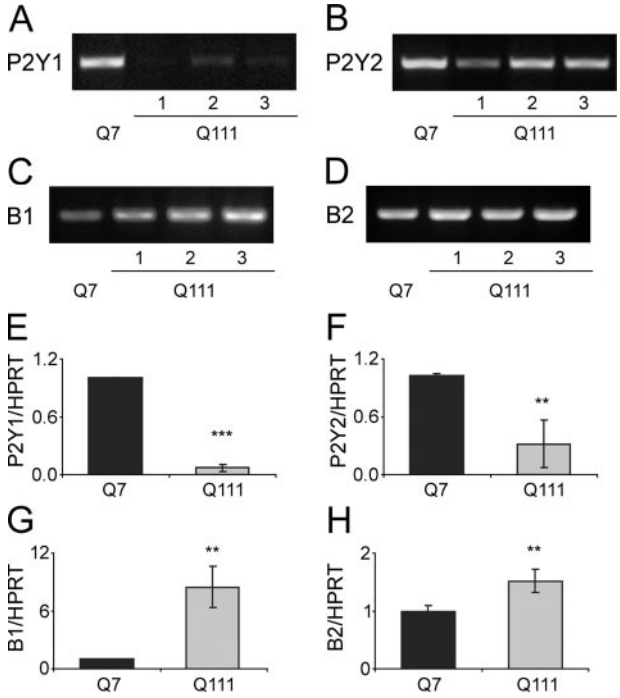

FIGURE 2. **Expression of P2Y and BK receptors in ST*Hdh*^{Q7} and ST*Hdh*^{Q111}.** Total RNA was extracted from one ST*Hdh*^{Q7} (*control*) (Q7, *black bars*) and three different ST*Hdh*^{Q111} mutant cell lines (Q111, 1–3, *gray bars*), reverse-transcribed, and subjected to PCR analysis. Semiquantitative PCR analysis of P2Y1 (*A*) and P2Y2 receptors (*B*), B1 (*C*), and B2 (*D*) receptors. Quantitative real-time PCR analysis of the expression of P2Y1 and P2Y2 receptors (*E* and *F*, respectively), and of B1 and B2 BK receptors (*G* and *H*, respectively). Data are given as the mean ± S.D., with differences significant at $p < 0.05$, *; $p < 0.01$, **; and $p < 0.001$, ***. HPRT, hypoxanthine-guanine phosphoribosyltransferase.

ST*Hdh*^{Q111} cells (45.10 ± 16.76 μM *versus* 11.24 ± 1.81 μM, $p = 6e\text{-}5$, Fig. 1*B*).

In contrast to ATP, the Ca^{2+} response to BK was higher in ST*Hdh*^{Q111} (1.40 ± 0.22 μM with respect to 1.20 ± 0.17 μM in ST*Hdh*^{Q7}cells, $p = 0.01$, Fig. 1*C*). In mitochondria the peaks were 35.44 ± 9.94 μM in control cells and 71.86 ± 18.76 μM, $p = 1.8e\text{-}8$, in mutant cells (Fig. 1*D*).

The Ca^{2+} content of the ER had no role in the differences between the cytoplasmic and mitochondrial responses in control and mutant cells, as the steady-state Ca^{2+} level measured with erAEQ did not differ significantly between ST*Hdh*^{Q7} and ST*Hdh*^{Q111} cells (225.73 ± 37.77 μM and 202.65 ± 42.71 μM, respectively, $p = 0.1$) (Fig. 1*E*).

Altered Expression of Purinergic and Bradykinin Receptors—The simplest explanation for the differences in ATP and BK-mediated Ca^{2+} signaling would be the different amounts of receptors expressed in control and mutant cells. The differences, however, could instead have been due to the clonal nature of the cells. The expression level of the two receptors was thus analyzed in the clone of Fig. 1 and in two additional clones (ST*Hdh*$^{Q111\text{-}2}$ and ST*Hdh*$^{Q111\text{-}3}$).

The transcripts of the two P2Y receptor subtypes present in mouse (P2Y1 and P2Y2, Ref. 30) were indeed detected in the cells (Fig. 2, *A* and *B*). Q-RT-PCR with primers specifically designed to obtain amplicons of about 100 bp revealed a striking (about 20-fold) down-regulation of the transcription of the P2Y1 gene and a less pronounced down-regulation of the P2Y2 gene (Fig. 2, *E* and *F*) in all mutant cell lines.

The transcripts of the B1 and B2 kinin receptors were instead up-regulated (Fig. 2, *C* and *D*). In the Q-RT-PCR analysis, the B1 transcript was 3–12-fold higher in the three mutant cell lines, that of the B2 receptor 1.4–1.6-fold higher (Fig. 2, *G* and *H*).

Ca^{2+} Homeostasis Dysfunction in STHdh^{Q111} *Cells*—The AEQ assay shown in Fig. 1 averaged Ca^{2+} transients in the total population of cells expressing AEQ. The differences between control and mutant cells could thus have been due to the reduced (or enhanced) number of responding cells. Because the amount of AEQ consumed by released Ca^{2+} was normalized to the total amount of expressed AEQ, if the population of cells responding to stimulation had been different in control and mutant cells, a correspondingly smaller portion of AEQ would have been used for the normalization. It was thus important to control the Ca^{2+} changes in single cell.

The analysis of the images in single cells loaded with Fura-2 (Fig. 3) revealed that ATP induced Ca^{2+} transients in 88% of ST*Hdh*^{Q7} cells, but only in 54% of the mutant ST*Hdh*^{Q111} cells (Fig. 3*D*). The peaks of the transients in responding mutant ST*Hdh*^{Q111} cells were 18% lower than in control cells (0.5 ± 0.23 *versus* 0.61 ± 0.11 normalized Fura-2 ratios (n.r.), $p =$

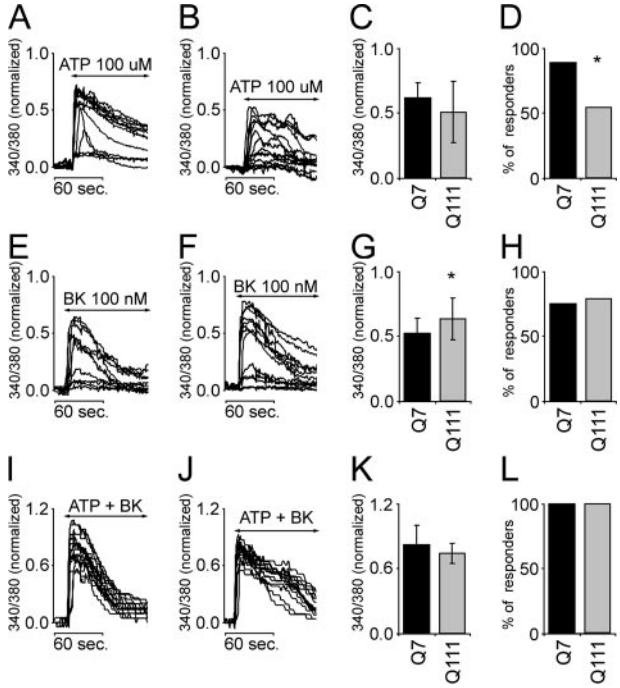

FIGURE 3. **Fura-2 measurements in ST*Hdh*^{Q7} and ST*Hdh*^{Q111} cells stimulated with ATP and BK.** ST*Hdh*^{Q7} (Q7, *black bars*) and ST*Hdh*^{Q111} (Q111, *gray bars*) cells were loaded with Fura-2 and stimulated with 100 μM ATP (*A–D*), with 100 nM BK (*E–H*), or with a mixture of 100 μM ATP and 100 nM BK (*I–L*). *Panels A*, *E*, *I* refer to Q7 cells, *panels B*, *F*, *J* to Q111 cells. The percentage of responding Q7 and Q111 cells after ATP stimulation is shown in *panel D*; when only the peaks of the Ca^{2+} transients of responding cells were compared, those in Q111 cells were lower at $p = 0.036$ for the case of ATP, and not significantly different for that of BK (*H*). With BK the peaks of the transients of responding cells were higher in Q111 cells than in Q7 cells (*G*, $p = 0.03$). When cells were stimulated with both ATP and BK the percentage of responding cells approached 100% and the height of peaks were not significantly different in Q7 and Q111 cells (*L*). Representative experiments for each condition are shown from six independent experiments for single agonist stimulation for each cell type and from four experiments for the stimulation with both ATP and BK for each cell type. The data are expressed as the mean ± S.D. Differences were significant at $p < 0.05$, *; $p < 0.01$, **; and $p < 0.001$, ***.

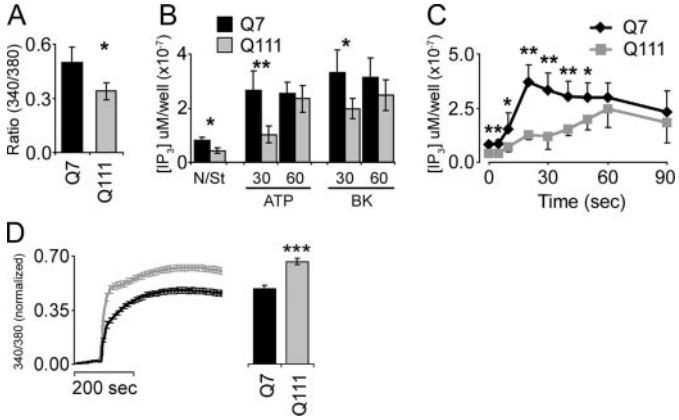

FIGURE 4. **$InsP_3$ dynamics in ST*Hdh*^{Q7} and ST*Hdh*^{Q111} cells stimulated with ATP and BK.** *A*, base line of $[Ca^{2+}]$ in nonstimulated ST*Hdh*^{Q111} (Q111, *gray bar*) and in ST*Hdh*^{Q7} cells (Q7, *black bar*, $p < 0.05$, $n = 10$ for each cell type). The measurement was done using Fura-2. *B*, Q7 (*black bars*) and Q111 cells (*gray bars*) were stimulated with either ATP or BK, and $InsP_3$ was extracted at the indicated time points. The extracts were subjected to an AlphaScreen $InsP_3$ assay to measure $InsP_3$. *N/St*, nonstimulated cells. *C*, Q7 (*black rectangles*) and Q111 (*gray squares*) cells were stimulated with a mixture of 100 μM ATP and 100 nM BK, and the $InsP_3$ levels were measured at the indicated times after stimulation. Data are expressed as the mean ± S.D. of at least three experiments. *D*, Q7 (*black bars*) and Q111 (*gray bars*) cells were loaded with Fura-2 and stimulated with 100 μM of iInsP3/PM (cell permeable derivative of $InsP_3$). Data are expressed as the mean ± S.E. of $n = 103$ for Q7 and $n = 129$ for Q111 cells in six independent experiments for each cell line. Differences were significant at $p < 0.05$, *; $p < 0.01$, **; and $p < 0.001$, ***.

0.036, Fig. 3*H*). Thus, a portion of the larger (60%) decrease in the height of the Ca^{2+} peaks detected in ST*Hdh*^{Q111} with AEQ had been due to the decreased number of responding cells. In the case of BK the number of cells-responders was instead essentially the same in control and mutant cells (76 and 74%, respectively). The increase in the height of the Ca^{2+} peak in mutant cells (0.62 ± 0.16 n.r.) with respect to control cells (0.51 ± 0.12 n.r., $p = 0.03$, 18%) was close to that seen with AEQ (16%). When cells were stimulated with both ATP and BK, all ST*Hdh*^{Q7} and ST*Hdh*^{Q111} cells in the population responded (Fig. 3*L*).

Dynamics of $InsP_3$ Production in STHdh^{Q111} Cells—The Fura-2 experiments had also shown that basal Ca^{2+} in non-stimulated ST*Hdh*^{Q111} cells was significantly lower than in control cells (43.3 ± 5.32 fluorescence units (f.u.) *versus* 63.7 ± 9.18 f.u., respectively, $p < 0.001$, Fig. 4*A*). This prompted a study of the $InsP_3$ levels. In line with the lower levels of basal Ca^{2+}, the $InsP_3$ level in non-stimulated cells was significantly lower in ST*Hdh*^{Q111} than in ST*Hdh*^{Q7} cells (Fig. 4*B*, *N/St*). The dynamics of $InsP_3$ production was then explored in cells stimulated with either ATP or BK. As shown in Fig. 4*B*, the production of $InsP_3$ was delayed in ST*Hdh*^{Q111} with respect to ST*Hdh*^{Q7} cells. It was much lower 30 s after stimulation with either ATP or BK, the difference only disappearing after 60 s. The difference was lower with BK. When cells were stimulated with both agonists (Fig. 4*C*), the increase in $InsP_3$ level was clearly delayed in mutant cells, reaching a maximum at 20 s in control cells, but only at 60 s in ST*Hdh*^{Q111} cells.

The higher BK-induced Ca^{2+} response may seem odd, considering the decreased rate of $InsP_3$ production in mutant cells. Possibly, the sensitivity of the $InsP_3$ receptors could have been changed in the mutants. Therefore, we explored the possibility directly by treating control and mutant cells with a membrane-permeable derivative of $InsP_3$ (i$InsP_3$/PM). The experiment showed that $InsP_3$ receptors in ST*Hdh*^{Q111} cells indeed were more sensitive then in ST*Hdh*^{Q7} cells (0.64 ± 0.019 n.r., *versus* 0.47 ± 0.018 n.r, respectively, $p < 0.001$, Fig. 4*D*). The result nicely confirmed previous data showing increased sensitivity of the $InsP_3$ receptors by mutant Htt (31).

Transcriptional Regulation of $InsP_3$ Controlling Enzymes—The slower rate of $InsP_3$ production in stimulated mutant cells prompted a study of the expression of the components of the PI cycle and of the $InsP_3$ receptors. The striatum of the KI-*Hdh*^{Q111} parent mouse was also studied. The transcripts of IMPA1 and inositol polyphosphatase, which are rate-limiting in the cycle, were down-regulated both in ST*Hdh*^{Q111} cells (by 40 and 20%, respectively, Fig. 5, *A* and *C*), and in the striatum (by 15 and 25%, respectively; Fig. 5, *B* and *D*).

Of the four PLCβ isoforms that hydrolyze PIP_2, only PLCβ3 was detected in the striatal cells, (in the striatum PLCβ1 was instead more abundant). The PLCβ3 transcript was up-regulated in ST*Hdh*^{Q111} cells, that of PLCβ1 in the striatum (Fig. 5, *E* and *F*). The transcript of the neuronal type $InsP_3$ receptor (type 1) was down-regulated in both the mutant cells and the

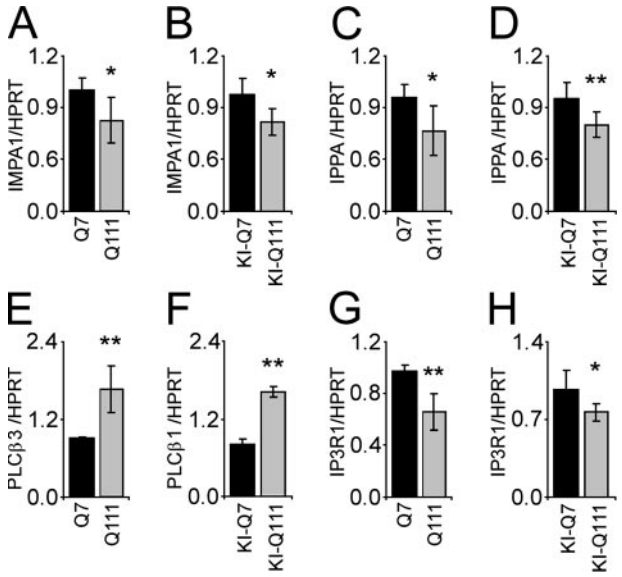

FIGURE 5. **mRNA of components of the PI cycle in clonal striatal cells and striatal tissues.** Total RNA was extracted from one ST*Hdh*^{Q7} (Q7, *black bars*) and three ST*Hdh*^{Q111} cell lines (Q111, 1–3, averaged and presented as Q111, *gray bars*) (*A*, *C*, *E*, *G*), and from striatal tissues of WT-*Hdh*^{Q7} and KI-*Hdh*^{Q111} mice (*B*, *D*, *F*, *H*). RNAs were quantified, reverse-transcribed and subjected to Q-RT-PCR analysis using specific primers for IMPA1 (*A* and *B*), inositol polyphosphatase (IPPA) (*C* and *D*), PLCβ3 (*E*), PLCβ1 (*F*), and $InsP_3R1$ (*G* and *H*). The data represent the mean ± S.D. for at least four PCRs from two independent retrotranscriptions for each condition. The differences were significant at $p < 0.05$, *; $p < 0.01$, **; and $p < 0.001$, ***. HPRT, hypoxanthine-guanine phosphoribosyltransferase.

striatum (Fig. 5, *G* and *H*), in line with previous studies showing that the expression of numerous signaling genes was dysregulated in mouse and cellular HD models, and in HD patients (32, 33).

Ca^{2+} Handling by Mitochondria in STHdh^{Q111} Cells—The driving force for mitochondrial Ca^{2+} uptake ($\Delta\psi_m$), was explored with the fluorescent probe TMRM (27) in peripheral mitochondria to avoid artifactual fluorescence changes due to variations in cellular thickness. Fig. 6*D* shows a minor, but significant (95.3% confidence, $p = 0.047$, unpaired 1-sided Student's *t* test) fluorescence difference between resting ST*Hdh*^{Q7} and ST*Hdh*^{Q111} cells (199.7 ± 18.6 f.u. *versus* 192.3 ± 16.4 f.u., data collected from more then 200 cells in 15 experiments for each cell type). When ST*Hdh*^{Q7} cells were preincubated with the complex II inhibitor 3-NPA, the fluorescence decreased by about 10% in control cells (180.2 ± 14.3 f.u. *versus* 199.7 ± 18.6 f.u., $p = 3e\text{-}15$), and by 18% in ST*Hdh*^{Q111} cells (158.7 ± 9.8 f.u. *versus* 192.3 ± 16.4 f.u., $p = 2.1e\text{-}61$). Ca^{2+} uptake was monitored directly in mitochondria within control and ST*Hdh*^{Q111} cells, which were permeabilized with digitonin to expose them to concentrations of free Ca^{2+} precisely controlled with EGTA. To increase the efficiency of AEQ expression and thus to improve the quality of the results, in these experiments the DNA of mtAEQ was transferred into the cells using lentiviral vectors pLV-mitAEQ. As shown in Fig. 6*A*, perfusion with an EGTA buffer generating 1.6 μM free Ca^{2+} induced a Ca^{2+} transient which peaked at 103.6 ± 33.5 μM in ST*Hdh*^{Q7} cells ($n = 11$) and at 86.7 ± 27.7 μM in ST*Hdh*^{Q111} cells ($n = 12$). The difference was not significant ($p = 0.1$). Perfusion with 11 μM free Ca^{2+} evoked a significantly higher mitochondrial Ca^{2+} uptake transient in ST*Hdh*^{Q7} cells (300.6 ± 28.4 μM, $n = 6$, Fig. 6*B*) than in ST*Hdh*^{Q111} cells (172.4 ± 36.0 μM, $n = 6$, $p = 0.00012$). At these two relatively low Ca^{2+} concentrations, 3-NPA had no effect on the transients in either cell type. At 71 μM Ca^{2+}, however, the peak (453.8 ± 18.6 μM, $n = 6$) was greatly reduced by 3-NPA (292.3 ± 53.2 μM, $n = 6$, $p = 0.0001$, Fig. 6*C*) in ST*Hdh*^{Q7} cells. In ST*Hdh*^{Q111} cells, the peak was much lower, (316.0 ± 25.6 μM, $n = 6$, $p = 1e\text{-}5$) and was decreased much more dramatically by 3-NPA (166.3 ± 16.8, $n = 6$, $p = 3.1e\text{-}6$). Thus, mitochondria in mutant cells were about as efficient in taking up Ca^{2+} as those in control cells when the concentration of the ion in the environment was low. As it increased, their ability to control Ca^{2+} decreased progressively in mutant cells, the difference being exacerbated if complex II was inhibited by 3-NPA.

The mitochondrial defect in HD neurons has been suggested to concern complex II. Even if no unambiguous proof of it has yet been obtained in the model cells used here, it was interesting to study whether the inhibition of the complex was specific in inducing mitochondrial damage ($\Delta\psi$ and Ca^{2+} uptake); i.e., whether other means of deenergizing mitochondria had the same effect as 3-NPA. ST*Hdh*^{Q7} and ST*Hdh*^{Q111} cells were thus treated with increasing concentrations of the uncoupler FCCP. As shown in Fig. 6*E* 0.8 μM FCCP decreased the $\Delta\psi_m$ by 33% in ST*Hdh*^{Q111} cells, but only by 6% in ST*Hdh*^{Q7} cells (p 2e-7, $n = 6$). Fig. 6*F* shows that the uncoupler decreased Ca^{2+} uptake more in the mitochondria of mutant cells than in those of the controls (65% *versus* 44%, $p = 0.0049$, $n = 5$ at 0.8 μM FCCP). Thus, mitochondria of mutant cells were more sensitive to deenergization in general, not only to that caused by inhibitors of complex II.

Mutant huntingtin, and 3-NPA, have been proposed to make the permeability transition pore (PTP) more sensitive to Ca^{2+} (16, 34–36). The preferential opening of the pore could explain the decrease of the membrane potential in the mitochondria of mutant cells challenged with high Ca^{2+} concentrations (Fig. 6, *B* and *C*). To test this possibility, the experiment of Fig. 6*B* was thus repeated in the presence of the PTP blocker CsA. When cells permeabilized with digitonin were perfused with a buffer containing 20 μM free Ca^{2+} the decrease of the $\Delta\psi$ was significantly more pronounced in mutant with respect to control cells (50%, $p < 0.0001$ *versus* 14%, $p < 0.025$, respectively). However, the $\Delta\psi$ in the mitochondria of mutant cells pretreated with CsA was not different from that of CsA-treated control cells, indicating that the greater decrease of $\Delta\psi$ in the mitochondria of mutant cells challenged with high Ca^{2+} concentration, was indeed due to the preferential opening of the PTP (Fig. 6*G*). Then experiments were performed to assess whether the preferential opening of PTP could have a role in the reduced mitochondrial Ca^{2+} uptake in ST*Hdh*^{Q111} (see Fig. 6*B*). Permeabilized cells transduced with the lentiviral vector pLV-mtAEQ were pretreated for 1 h with CsA (10 μM), and then perfused with a buffer containing 20 μM free Ca^{2+}. As shown in Fig. 6*H*, the pretreatment completely abolished the decrease in mitochondrial Ca^{2+} uptake in mutant cells when challenged with a high Ca^{2+} concentration. Interestingly, the height of the peaks of the CsA-treated ST*Hdh*^{Q7} and ST*Hdh*^{Q111} cells (421.88 ±

63.52 μM and 407.04 ± 92.42 μM, $p = 0.45$), was even higher than those of the respective nontreated controls (306.13 ± 46.63 μM, $p = 0.05$ in ST*Hdh*^{Q7} cells, 228.54 ± 22.62 μM, $p = 0.0052$ in ST*Hdh*^{Q111} cells). Thus the PTP of mitochondria in mutant cells indeed was more sensitive to Ca^{2+}.

Transcriptional Regulation of ROS-scavenging Enzymes—Huntingtin generates ROS in the striata of a HD mouse model, and 3-NPA, which generates ROS, does so in PC12 cells (37, 38). The level of ROS was thus explored in control and mutant striatal cells. Because a first set of experiments on the mutant cell clone employed in most of the work had failed to reveal differences in ROS level between mutant and control cells, the study was extended to two other mutant cell clones (ST*Hdh*$^{Q111\text{-}2}$ and ST*Hdh*$^{Q111\text{-}3}$). In all mutant clones, the concentration of ROS did not differ from the controls. However, when the cells were exposed to 3-NPA, the concentration of ROS increased as expected both in control and mutant cells. However, the increase was much more significant (even if variable) in the latter (Fig. 7*A*, $p = 0.012$, $n = 4$).

The transcription of the genes involved in the breakdown of ROS (Gpx1, catalase, SOD1, and SOD2) was analyzed next in the three independently generated ST*Hdh*^{Q111} clones (Fig. 7, *B–D*). The transcripts were up-regulated by 30–100% in all three mutant clones (most significantly in clone ST*Hdh*$^{Q111\text{-}2}$), with the exception of SOD2, which was instead unchanged (not shown). Pilot experiments on the transcription of the ROS genes in the striata of the KI-*Hdh*^{Q111} mice have so far failed to yield sufficiently reproducible results (not shown).

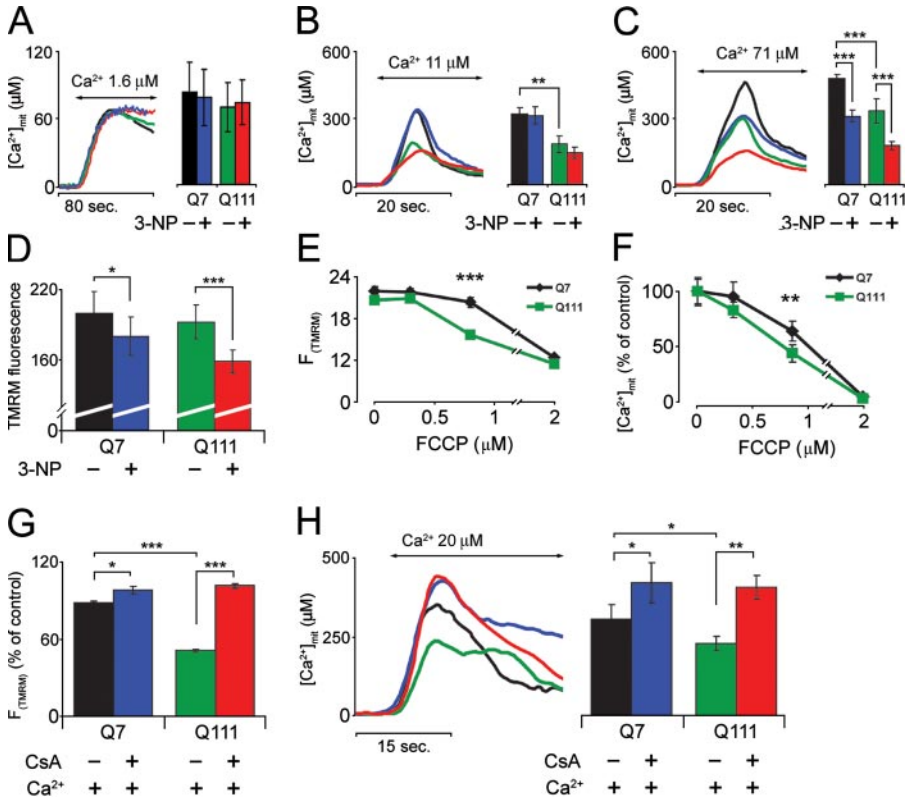

FIGURE 6. **Mitochondrial membrane potential and Ca^{2+} uptake in ST*Hdh*^{Q7} and ST*Hdh*^{Q111} cells.** To measure Ca^{2+} cells were transduced with mitAEQ using lentiviral vectors. After AEQ reconstitution, cells were permeabilized with10 μM digitonin (2 min) and perfused with Ca^{2+}-EGTA buffers containing 1.6 (*A*), 11 (*B, G, H,* and *I*), or 71 (*C*) μM free Ca^{2+}. *D*, ST*Hdh*^{Q7} (Q7, *black bar*) and ST*Hdh*^{Q111} (Q111, *green bar*) cells were loaded with TMRM and the fluorescence of peripheric mitochondria was estimated with a CCD camera. The difference between Q7 and Q111 cells was significant at $p = 0.047$ (unpaired one-sided Student's *t* test). Pretreatment with 3-NPA (20 mM, 40 h) reduced the fluorescence (10% in Q7 cells, *blue bar*, and 18% in Q111 cells, *red bar*). Data expressed as the mean ± S.D. (about 200 cells from 15 experiments for each cell type) for untreated cells and cells pretreated with 3-NPA (about 80–100 cells from six experiments for each cell type). *E*, cells were loaded with TMRM and treated with the indicated concentrations of FCCP. The fluorescence was estimated with a CCD camera. The SD of fluorescence (27) was analyzed before and after FCCP addition. The data represent the mean ± S.D. of six experiments for each cell type. *F*, cells expressing mtAEQ were permeabilized and perfused with an EGTA buffer containing 11 μM free Ca^{2+} and the indicated concentrations of FCCP. The data represent the mean ± S.D. of five independent experiments for each condition. *G* and *H*, control (Q7) and mutant cells (Q111) were pretreated for 1 h with CsA (10 μM, *blue* and *red bars*) and then perfused with buffer containing 20 μM free Ca^{2+}. The SD of TMRM fluorescence (27) was analyzed (*G*), and mitochondrial calcium (*H*) was measured in cells transduced with pLV-mitAEQ (see detailed description under "Experimental Procedures"). The data are presented as mean ± S.E. of 4–6 independent experiments for each condition. Differences were significant at $p < 0.05$, *; $p < 0.01$, **; and $p < 0.001$, ***.

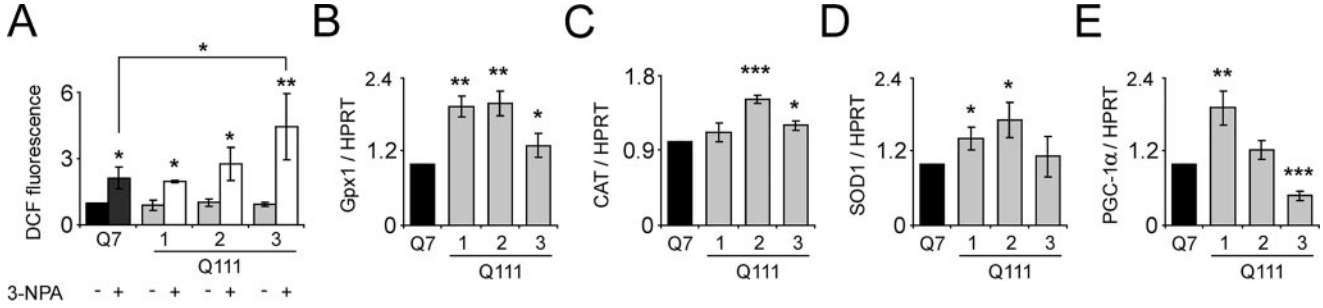

FIGURE 7. **ROS in striatal cells and tissues of the mouse HD model.** *A*, ST*Hdh*^{Q7} (Q7, *black bars*) and ST*Hdh*^{Q111} (Q111, *light gray bars*) cells were loaded with 2′,7′-dichlorodihydrofluorescein diacetate (DCF) and the fluorescence of oxidized fluorescein was measured with a spectrophotometer. 3-NPA (10 mM) was added 40 h before the experiment. Total RNA was extracted from Q7 (*black bars*) and Q111 cells (*gray bars*, *B–E*), and RNAs were quantified, reverse-transcribed and subjected to Q-RT-PCR analysis using specific primers for the Gpx1 (*B*), catalase (*C*), SOD1 (*D*), and PGC-1α (*E*). The data represent the mean ± S.D. for at least three experiments. The differences were significant at $p < 0.05$, *; $p < 0.01$, **; and $p < 0.001$, ***. HPRT, hypoxanthine-guanine phosphoribosyltransferase.

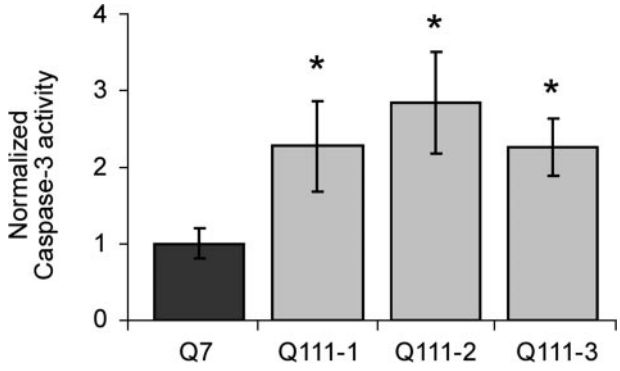

FIGURE 8. **Caspase-3 activity measurement as an indication of apoptosis.** The experiment was performed on ST*Hdh*^{Q7} cells (Q7, *black bars*) and on cells from three different mutant clones ST*Hdh*$^{Q111-1}$, ST*Hdh*$^{Q111-2}$, and ST*Hdh*$^{Q111-3}$ (Q111, 1–3 *gray bars*). Data represent the mean ± S.D. of three independent experiments performed in triplicate.

The recent observation that the transcription of the PGC-1α gene was specifically repressed in a ST*Hdh*^{Q111} cell clone (21) prompted an investigation of the interplay between the transcription of the PGC-1α gene, and that of the genes of ROS-scavenging enzymes. The study was performed in the three independently generated ST*Hdh*^{Q111} cell clones. The results (Fig. 7*E*) showed great variability in the amounts of PGC-1α transcripts in the three clones. No convincing correlation was found between the levels of transcription of the PGC-1α gene and those of the 3 genes for the ROS-scavenging enzymes. In the mutant clone used in most of the experiments described here the transcript of PGC-1α increased markedly with respect to control cells (by 1.92 ± 0.27-fold, $p = 0.0045$), as did those of the ROS-scavenging enzymes (see Fig. 7, *B–D*). In another clone the amount of the PGC-1α transcript increased only marginally (by 1.23 ± 0.15-fold, $p = 0.056$), whereas those of the ROS-scavenging enzymes instead increased markedly. In the third clone the amount of PGC-1α transcript decreased sharply with respect to control cells (by 0.48 ± 0.083-fold, $p = 0.0004$), whereas those of the ROS-scavenging enzymes either increased or remained essentially unchanged. Direct measurement of ROS (Fig. 7*A*) showed that the increase in their concentration induced by 3-NPA did not correlate convincingly with the levels of the transcripts of the scavenging enzymes nor with that of PGC-1α. Evidently, the dynamics of ROS generation/degradation in the mutant cells was not exclusively controlled by transcriptional effects.

Susceptibility of STHdh^{Q111} *Cells to Apoptosis*—HD neurons have particular propensity to succumb by apoptosis (39, 40), and the model cell line used in this contribution has been claimed to be selectively vulnerable to treatments that cause non-apoptotic death (16). The vulnerability of three mutant cell lines to apoptotic treatments was thus investigated. Fig. 8 shows that the tendency to undergo apoptosis after treatment with the classical apoptotic agent staurosporin (10 μM for 6 h) was significantly greater in all three mutant cell lines (by 2.28 ± 0.59-, 2.84 ± 0.66-, 2.26 ± 0.37-fold in ST*Hdh*$^{Q111-1}$, ST*Hdh*$^{Q111-2}$, and ST*Hdh*$^{Q111-3}$ cells, respectively) in respect with ST*Hdh*^{Q7} cells ($p < 0.05$ for all cases).

DISCUSSION

The accumulation of the expanded poly-Q fragments of Htt in the cytoplasm, nuclei, and axons is a hallmark of HD. As mentioned in the Introduction, the reasons for the preferential vulnerability of GABAergic MSNs to Htt, which is widely expressed in the brain and the body, is still an open problem. Mutant Htt aggregates are widely discussed with respect to their role in causing cell damage, and have even been claimed to decrease cell death risk in striatal neurons (41). Thus, they may have a number of functions, the dysregulation of the transcription of genes necessary for the function and eventual survival of striatal neurons now emerging as the most important (32, 33, 42–44). Transcription in HD neurons, however, could also be dysregulated by other agents, *e.g.* by ROS, the effect of the poly-Q aggregates being possibly linked to the late stages of the disease.

ROS have long been known to directly damage mitochondria: they dissipate the $\Delta\psi_m$, impairing the production of ATP, and preferentially damage mitochondrial DNA (18, 45–47). The mitochondrial dysfunction mediated by ROS has received new impulse from recent work showing that in HD striata, and even in the model cells used in this work, a transcriptional co-activator of the genes of ROS-scavenging enzymes (PGC-1α) is transcriptionally down-regulated (21). The down-regulation has been suggested to be important in the damage to striatal neurons: however, the experiments presented here have shown that the level of PGC-1α transcript is but one of the factors active in the regulation of the level of ROS, as it does not correlate with those of the ROS-scavenging enzymes in the model cells used here.

The discovery that inhibitors of mitochondrial complex II induce cell death in striatal neurons, and produce neuronal degeneration in the striatum *in vivo* (11) was an important development. Complex II inhibitors, as all other mitochondrial damaging agents, also generate ROS, emphasizing their potential role in the damage to HD neurons. The finding that the complex II inhibitor 3-NPA mimics the effects of mutant Htt is an indication that somehow links the inhibition of the complex to the latter. The matter, however, still has unclear facets: recent work on cultured striatal neurons transfected with an expanded poly-Q tract have shown no down-regulation of the mRNA of two components of complex II, but have instead documented a down-regulation of their proteins (48). It thus appears probable that complex II is defective in HD neurons due to some post-transcriptional (proteolytic) effect. Whether the complex is also defective in the cell model used here is an open question. In Htt neurons the defect of complex II would not only generate ROS, but would also make mitochondria less able to respond to requests for increased activity of the respiratory chain. The defect would of course be exacerbated if the function of complex II would be further depressed by inhibitors. The canonical endogenous inhibitor of the complex is malonic acid, which has frequently been used to induce neuronal degeneration (49–51). Work now in progress in our laboratory explores the possible increase of malonic acid in Htt neurons.

The work described here has shown that the mitochondrial damage in cells expressing mutant Htt only becomes evident

when mitochondria are exposed to stressing insults. Mitochondria in HD neurons thus appear to be in a borderline situation: this is also indirectly shown by experiments in which the parenteral administration of doses of 3-NPA that would not produce striatal damage it rats, induced instead striatal neurodegeneration when combined with sub-toxic doses of amphetamine (52). ROS would be likely candidates as the stressing agent(s) that would make the silent mitochondrial damage fully expressed, but Ca^{2+} could be an equally plausible candidate, given its accepted role as a mediator of neuronal damage (12, 13). Ca^{2+} signaling defects have indeed been a recurring theme in HD research (17, 53–55). Recent work has shown that the mitochondrial $\Delta\psi$ in cells expressing mutant Htt was particularly vulnerable to Ca^{2+} (17, 34), and poly-Q constructs have been found to preferentially deenergize mitochondria exposed to Ca^{2+} (17). However, the work presented here has shown that the damaging effect of Ca^{2+} was not due to the overloading of mitochondria with it. The damage appears instead to be linked to the continuous leakage of accumulated Ca^{2+}, incompletely compensated by the activity of the uptake uniporter made insufficient by the decrease of the $\Delta\psi$. The $\Delta\psi$ of mutant mitochondria would be able to sustain the accumulation of a Ca^{2+} pulse only lasting a short time, but not that of Ca^{2+} persistently increased in their environment. As suggested by others, and directly confirmed in the present work (Fig. 6, *G* and *H*), it appears likely that the increased sensitivity of the PTP to Ca^{2+} is critical to the inability of mitochondria to retain Ca^{2+}, thus triggering the increased Ca^{2+} cycling and eventual ATP deprivation. Naturally, the drainage of ATP would have dire consequences for cell life. Peri-mitochondrial Ca^{2+} could also increase by an additional mechanism because mutant Htt and the huntingtin-associated protein HAP1A form a ternary complex with the $InsP_3$ receptor, potentiating its Ca^{2+} releasing activity (31, 56) and exposing mitochondria to persistently high Ca^{2+} concentrations (57).

In summary, HD mitochondria appear to be more vulnerable to stress. Once stressed, they become peculiarly deenergized, with obvious deleterious consequences for the life of the neurons. Ca^{2+} and ROS are the most plausible inducers of such mitochondrial stress. The alterations of the transcription of the enzymes that control their homeostasis are important actors in their modulation in HD neurons. In the cell model described here the transcriptional alterations in the proteins that control the Ca^{2+} signal are likely to be operational on a longer time scale. The resulting alterations of Ca^{2+} homeostasis could reflect a compensatory mechanism developed by the cells to prevent, or at least to delay, Ca^{2+} from increasing to the levels that would fatally harm their mitochondria, making their silent damage fully evident.

REFERENCES

1. The Huntington's Disease Collaborative Research Group (1993) *Cell* **72,** 971–983
2. Sieradzan, K. A., and Mann, D. M. (2001) *Neuropathol Appl. Neurobiol.* **27,** 1–21
3. Cattaneo, E., Zuccato, C., and Tartari, M. (2005) *Nat. Rev. Neurosci.* **6,** 919–930
4. Bezprozvanny, I., and Hayden, M. R. (2004) *Biochem. Biophys. Res. Commun.* **322,** 1310–1317
5. Lin, M. T., and Beal, M. F. (2006) *Nature* **443,** 787–795
6. Browne, S. E., Bowling, A. C., MacGarvey, U., Baik, M. J., Berger, S. C., Muqit, M. M., Bird, E. D., and Beal, M. F. (1997) *Ann. Neurol.* **41,** 646–653
7. Browne, S. E., and Beal, M. F. (2004) *Neurochem Res.* **29,** 531–546
8. Milakovic, T., and Johnson, G. V. (2005) *J. Biol. Chem.* **280,** 30773–30782
9. Seong, I. S., Ivanova, E., Lee, J. M., Choo, Y. S., Fossale, E., Anderson, M., Gusella, J. F., Laramie, J. M., Myers, R. H., Lesort, M., and MacDonald, M. E. (2005) *Hum. Mol. Genet.* **14,** 2871–2880
10. Brouillet, E., Jacquard, C., Bizat, N., and Blum, D. (2005) *J. Neurochem.* **95,** 1521–1540
11. Beal, M. F., Brouillet, E., Jenkins, B. G., Ferrante, R. J., Kowall, N. W., Miller, J. M., Storey, E., Srivastava, R., Rosen, B. R., and Hyman, B. T. (1993) *J. Neurosci.* **13,** 4181–4192
12. Schwab, B. L., Guerini, D., Didszun, C., Bano, D., Ferrando-May, E., Fava, E., Tam, J., Xu, D., Xanthoudakis, S., Nicholson, D. W., Carafoli, E., and Nicotera, P. (2002) *Cell Death Differ.* **9,** 818–831
13. Bano, D., Young, K. W., Guerin, C. J., Lefeuvre, R., Rothwell, N. J., Naldini, L., Rizzuto, R., Carafoli, E., and Nicotera, P. (2005) *Cell* **120,** 275–285
14. Burnstock, G. (2006) *Trends Pharmacol. Sci.* **27,** 166–176
15. Leeb-Lundberg, L. M., Marceau, F., Muller-Esterl, W., Pettibone, D. J., and Zuraw, B. L. (2005) *Pharmacol. Rev.* **57,** 27–77
16. Ruan, Q., Lesort, M., MacDonald, M. E., and Johnson, G. V. (2004) *Hum. Mol. Genet.* **13,** 669–681
17. Panov, A. V., Gutekunst, C. A., Leavitt, B. R., Hayden, M. R., Burke, J. R., Strittmatter, W. J., and Greenamyre, J. T. (2002) *Nat. Neurosci.* **5,** 731–736
18. Wang, J., Green, P. S., and Simpkins, J. W. (2001) *J. Neurochem.* **77,** 804–811
19. Lin, J., Wu, P. H., Tarr, P. T., Lindenberg, K. S., St-Pierre, J., Zhang, C. Y., Mootha, V. K., Jager, S., Vianna, C. R., Reznick, R. M., Cui, L., Manieri, M., Donovan, M. X., Wu, Z., Cooper, M. P., Fan, M. C., Rohas, L. M., Zavacki, A. M., Cinti, S., Shulman, G. I., Lowell, B. B., Krainc, D., and Spiegelman, B. M. (2004) *Cell* **119,** 121–135
20. Leone, T. C., Lehman, J. J., Finck, B. N., Schaeffer, P. J., Wende, A. R., Boudina, S., Courtois, M., Wozniak, D. F., Sambandam, N., Bernal-Mizrachi, C., Chen, Z., Holloszy, J. O., Medeiros, D. M., Schmidt, R. E., Saffitz, J. E., Abel, E. D., Semenkovich, C. F., and Kelly, D. P. (2005) *PLoS Biol.* **3,** e101
21. Cui, L., Jeong, H., Borovecki, F., Parkhurst, C. N., Tanese, N., and Krainc, D. (2006) *Cell* **127,** 59–69
22. Weydt, P., Pineda, V. V., Torrence, A. E., Libby, R. T., Satterfield, T. F., Lazarowski, E. R., Gilbert, M. L., Morton, G. J., Bammler, T. K., Strand, A. D., Cui, L., Beyer, R. P., Easley, C. N., Smith, A. C., Krainc, D., Luquet, S., Sweet, I. R., Schwartz, M. W., and La Spada, A. R. (2006) *Cell Metab.* **4,** 349–362
23. Trettel, F., Rigamonti, D., Hilditch-Maguire, P., Wheeler, V. C., Sharp, A. H., Persichetti, F., Cattaneo, E., and MacDonald, M. E. (2000) *Hum. Mol. Genet.* **9,** 2799–2809
24. Zuccato, C., and Cattaneo, E. (2007) *Prog. Neurobiol.* **81,** 294–330
25. Brini, M., Marsault, R., Bastianutto, C., Alvarez, J., Pozzan, T., and Rizzuto, R. (1995) *J. Biol. Chem.* **270,** 9896–9903
26. Pfaffl, M. W. (2001) *Nucleic Acids Res.* **29,** e45
27. Duchen, M. R., Surin, A., and Jacobson, J. (2003) *Methods Enzymol.* **361,** 353–389
28. Follenzi, A., and Naldini, L. (2002) *Methods Mol. Med.* **69,** 259–274
29. Scemes, E., Duval, N., and Meda, P. (2003) *J. Neurosci.* **23,** 11444–11452
30. von Kugelgen, I., and Wetter, A. (2000) *Naunyn Schmiedebergs Arch Pharmacol.* **362,** 310–323
31. Tang, T. S., Tu, H., Chan, E. Y., Maximov, A., Wang, Z., Wellington, C. L., Hayden, M. R., and Bezprozvanny, I. (2003) *Neuron* **39,** 227–239
32. Luthi-Carter, R., Strand, A., Peters, N. L., Solano, S. M., Hollingsworth, Z. R., Menon, A. S., Frey, A. S., Spektor, B. S., Penney, E. B., Schilling, G., Ross, C. A., Borchelt, D. R., Tapscott, S. J., Young, A. B., Cha, J. H., and Olson, J. M. (2000) *Hum. Mol. Genet.* **9,** 1259–1271
33. Kuhn, A., Goldstein, D. R., Hodges, A., Strand, A. D., Sengstag, T., Kooperberg, C., Becanovic, K., Pouladi, M. A., Sathasivam, K., Cha, J. H., Hannan, A. J., Hayden, M. R., Leavitt, B. R., Dunnett, S. B., Ferrante, R. J., Albin, R., Shelbourne, P., Delorenzi, M., Augood, S. J., Faull, R. L., Olson, J. M., Bates, G. P., Jones, L., and Luthi-Carter, R. (2007) *Hum. Mol. Genet.* **16,** 1845–1861

34. Milakovic, T., Quintanilla, R. A., and Johnson, G. V. (2006) *J. Biol. Chem.* **281,** 34785–34795
35. Choo, Y. S., Johnson, G. V., MacDonald, M., Detloff, P. J., and Lesort, M. (2004) *Hum. Mol. Genet.* **13,** 1407–1420
36. Sawa, A., Wiegand, G. W., Cooper, J., Margolis, R. L., Sharp, A. H., Lawler, J. F., Jr., Greenamyre, J. T., Snyder, S. H., and Ross, C. A. (1999) *Nat. Med.* **5,** 1194–1198
37. Perez-Severiano, F., Santamaria, A., Pedraza-Chaverri, J., Medina-Campos, O. N., Rios, C., and Segovia, J. (2004) *Neurochem. Res.* **29,** 729–733
38. Mandavilli, B. S., Boldogh, I., and Van Houten, B. (2005) *Brain Res. Mol. Brain Res.* **133,** 215–223
39. Tang, T. S., Slow, E., Lupu, V., Stavrovskaya, I. G., Sugimori, M., Llinas, R., Kristal, B. S., Hayden, M. R., and Bezprozvanny, I. (2005) *Proc. Natl. Acad. Sci. U. S. A.* **102,** 2602–2607
40. Shehadeh, J., Fernandes, H. B., Zeron Mullins, M. M., Graham, R. K., Leavitt, B. R., Hayden, M. R., and Raymond, L. A. (2006) *Neurobiol. Dis.* **21,** 392–403
41. Steffan, J. S., Agrawal, N., Pallos, J., Rockabrand, E., Trotman, L. C., Slepko, N., Illes, K., Lukacsovich, T., Zhu, Y. Z., Cattaneo, E., Pandolfi, P. P., Thompson, L. M., and Marsh, J. L. (2004) *Science* **304,** 100–104
42. Jiang, H., Nucifora, F. C., Jr., Ross, C. A., and DeFranco, D. B. (2003) *Hum. Mol. Genet.* **12,** 1–12
43. Nucifora, F. C., Jr., Sasaki, M., Peters, M. F., Huang, H., Cooper, J. K., Yamada, M., Takahashi, H., Tsuji, S., Troncoso, J., Dawson, V. L., Dawson, T. M., and Ross, C. A. (2001) *Science* **291,** 2423–2428
44. Zhai, W., Jeong, H., Cui, L., Krainc, D., and Tjian, R. (2005) *Cell* **123,** 1241–1253
45. Salazar, J. J., and Van Houten, B. (1997) *Mutat. Res.* **385,** 139–149
46. Santos, J. H., Hunakova, L., Chen, Y., Bortner, C., and Van Houten, B. (2003) *J. Biol. Chem.* **278,** 1728–1734
47. Yakes, F. M., and Van Houten, B. (1997) *Proc. Natl. Acad. Sci. U. S. A.* **94,** 514–519
48. Benchoua, A., Trioulier, Y., Zala, D., Gaillard, M. C., Lefort, N., Dufour, N., Saudou, F., Elalouf, J. M., Hirsch, E., Hantraye, P., Deglon, N., and Brouillet, E. (2006) *Mol. Biol. Cell* **17,** 1652–1663
49. Greene, J. G., and Greenamyre, J. T. (1995) *J. Neurochem.* **64,** 430–436
50. Lorenc-Koci, E., Golembiowska, K., and Wardas, J. (2005) *Brain Res.* **1051,** 145–154
51. Maragos, W. F., Young, K. L., Altman, C. S., Pocernich, C. B., Drake, J., Butterfield, D. A., Seif, I., Holschneider, D. P., Chen, K., and Shih, J. C. (2004) *Neurochem Res.* **29,** 741–746
52. Bowyer, J. F., Clausing, P., Schmued, L., Davies, D. L., Binienda, Z., Newport, G. D., Scallet, A. C., and Slikker, W., Jr. (1996) *Brain Res.* **712,** 221–229
53. Goffredo, D., Rigamonti, D., Tartari, M., De Micheli, A., Verderio, C., Matteoli, M., Zuccato, C., and Cattaneo, E. (2002) *J. Biol. Chem.* **277,** 39594–39598
54. Cepeda, C., Ariano, M. A., Calvert, C. R., Flores-Hernandez, J., Chandler, S. H., Leavitt, B. R., Hayden, M. R., and Levine, M. S. (2001) *J. Neurosci. Res.* **66,** 525–539
55. Zeron, M. M., Hansson, O., Chen, N., Wellington, C. L., Leavitt, B. R., Brundin, P., Hayden, M. R., and Raymond, L. A. (2002) *Neuron* **33,** 849–860
56. Tang, T. S., Tu, H., Orban, P. C., Chan, E. Y., Hayden, M. R., and Bezprozvanny, I. (2004) *Eur. J. Neurosci.* **20,** 1779–1787
57. Brini, M. (2003) *Cell Calcium* **34,** 399–405